Penetration depth in conventional layered superconductors: A proximity-effect model

S. P. Zhao and Q. S. Yang
Institute of Physics and Center for Condensed Matter Physics, Chinese Academy of Sciences, Beijing 100080, People's Republic of China
(Received 12 January 1999)

We propose a theory for the penetration depth $\lambda(T)$ of superconducting bilayers and multilayers, which are composed of two dissimilar superconducting layers S and S' with arbitrary coupling strength, and with the S layer thickness ($T_{c,S} > T_{c,S'}$) less than or comparable to its coherence length. Within the framework of the theory, we discuss the influences of the S' layer parameters, and of the coupling strength between the S' and S layers. We show that their variations lead to a variety of temperature dependences of $\lambda(T)$. Many of the basic features observed experimentally in conventional SS' structures have been reproduced. The theory begins with an extension of the proximity-effect model developed by Golubov *et al.* [Phys. Rev. B **51**, 1073 (1995)], which is based on the Usadel equations. It therefore applies to the dirty SS' system, and provides a description of the superconducting properties over the entire temperature range below T_c, the transition temperature of the system. We shall compare our model with a phenomenological model developed within the proximity-effect theory which is applicable near T_c. A brief discussion on the highly anisotropic systems in connection with the intrinsically layered high-T_c superconductors is also presented. [S0163-1829(99)05923-8]

I. INTRODUCTION

Magnetic penetration depth $\lambda(T)$ of superconducting bilayers[1–4] and multilayers[5] is known to have temperature dependences that are quite different from those of bulk BCS superconductors. In particular, recent measurements on Nb/Al,[1] Nb/Cu,[2,3] and NbN/Al (Ref. 3) bilayer structures indicate that in a wide temperature range, the $\lambda(T)$ curve can have a linear or sublinear temperature dependence, or obey a power law.[6] These results deviate substantially from the BCS exponential behavior (at low temperatures), and are believed to be associated with the spatial variations of the superconducting properties. In an earlier attempt to explain these phenomena, Pambianchi, Mao, and Anlage[7] proposed a phenomenological model utilizing the proximity-effect theory which is based upon the linearized self-consistency equation for the order parameter.[8,9] Similar treatment was also used by Claassen *et al.* in Ref. 3.

From these studies on SN (superconductor/normal metal) or SS' (we set $T_{c,S'} < T_{c,S}$ throughout this paper) structures, it appears that the variations of the sample and material parameters of the N or S' layers and their coupling strength to the S layers greatly affect the experimental observations. This can be understood in part from the following simple cases. Let us consider the in-plane penetration depth $\lambda_{ab}(T)$ of an SS' structure. If the coupling between S and S' is sufficiently weak so that they are not affected by each other, one expects a clear two-gap structure in the $\lambda_{ab}(T)$ curve. Namely, it undergoes a faster decrease around and below $T_{c,S'}$, which is a result of the onset of superconductivity in S'. When the coupling increases, such a feature should again be obvious if the S' layer thickness $d_{S'}$ is much larger compared to its coherence length $\xi_{S'}$, since in this case, much part across $d_{S'}$ remains unaffected. For less extreme cases, the $\lambda_{ab}(T)$ curve is expected to become ''smoother,'' but to decrease with decreasing temperature in a way that should differ from the behavior of a single BCS superconductor. Apparently, the magnitude of $T_{c,S'}$ relative to $T_{c,S}$ should play an important role in the overall shape of the $\lambda_{ab}(T)$ curve.

In this paper, starting from an extension of the proximity-effect model developed by Golubov and co-workers,[10,11] we present an approach for the calculations of both in-plane and out-of-plane penetration depths in SS' bilayers and multilayers, which takes the above considerations into account. The properties of SN systems are discussed in the limit as $T_{c,S'} \rightarrow 0$. In our model, we assume that the S' layer thickness is arbitrary, while the S layer thickness should be less than or comparable to its coherence length. The coupling strength between S and S' layers is arbitrary, and is equal on each interface for a multilayer. Based upon our approach, we shall discuss the roles of the thickness, resistivity, and transition temperature of the S' layers, and of their coupling strength to the S layers. We shall show that our model leads to a variety of temperature dependences of $\lambda(T)$, from which many of the basic features experimentally observed[1–5] can be reproduced.

The present model is based upon the Usadel equations,[12] which are the dirty-limit version of Eilenberger's theory.[13] Therefore our theory applies to the dirty SS' systems. For the systems to which the theory applies, it provides a description of the superconducting properties over the entire temperature range below T_c, the transition temperature of the system. We shall compare our results with those predicted by the phenomenological model of Pambianchi, Mao, and Anlage,[7] which is strictly valid only near T_c.

A frequently observed feature of $\lambda_{ab}(T)$ in the intrinsically layered high-T_c superconductors[14] has been its linear and quadratic temperature dependences at low and very low temperatures,[15,16] which are often interpreted in terms of impurity scattering[17] or nonlocal effects[18] for a d-wave superconductor. This linear plus quadratic feature is also obtained in our calculations in certain parameter range. Although the high-T_c superconductors can hardly be described by the

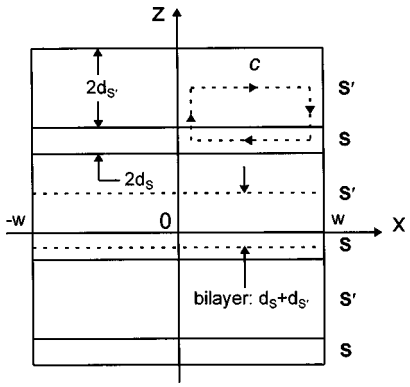

FIG. 1. An SS' multilayer system with constituent layer thicknesses of $2d_S$ and $2d_{S'}$, and $T_{c,S'}<T_{c,S}$. Due to its symmetric configuration, it is sufficient to discuss the bilayer in the region $-d_S<z<d_{S'}$, as indicated by two dashed lines, for our model calculation. The rectangular contour c is used to derive $\lambda_c(T)$ in Eq. (23) for the multilayer slab with thickness of $2w$. The slab is supposed to be infinite in both y and z directions.

present simple s-wave SS' multilayer, our results indicate that the proximity effect may play an important role in the $\lambda(T)$ behavior of these materials, a point already suggested by Pambianchi, Mao, and Anlage,[7] by Adrian *et al.*,[19] and by Klemm and Liu.[20]

The paper proceeds as follows. We first present the basic equations for dirty SS' layered superconductors and make the thin S layer approximation. Then T_c is evaluated in two different ways, from which we discuss the validity of the approximation made. Next, we compute both in-plane and out-of-plane penetration depths and present the numerical results, which are then compared with the phenomenological model of Pambianchi, Mao, and Anlage.[7] Finally, a brief discussion in connection with the highly anisotropic superconducting multilayers and high-T_c cuprates is presented.

II. BASIC EQUATIONS FOR SS' LAYERED SUPERCONDUCTORS AND THIN S LAYER APPROXIMATION

In Fig. 1 we show a multilayer with constituent layer thicknesses of $2d_{S,S'}$. Due to the symmetric configuration, it is sufficient to consider the bilayer confined between the two dashed lines, and the Usadel equations can be written as[10,11]

$$\Phi_{S'}=\Delta_{S'}+\xi_{S'}^2\frac{1}{\omega_n G_{S'}}(G_{S'}^2\Phi_{S'}')', \tag{1a}$$

$$\Delta_{S'}\ln\frac{T}{T_{c,S'}}+2\frac{T}{T_c}\sum_{\omega_n}\frac{\Delta_{S'}-\Phi_{S'}G_{S'}}{\omega_n}=0, \tag{1b}$$

for $0<z<d_{S'}$, and

$$\Phi_S=\Delta_S+\xi_S^2\frac{1}{\omega_n G_S}(G_S^2\Phi_S')', \tag{2a}$$

$$\Delta_S\ln\frac{T}{T_{c,S}}+2\frac{T}{T_c}\sum_{\omega_n}\frac{\Delta_S-\Phi_S G_S}{\omega_n}=0, \tag{2b}$$

for $-d_S<z<0$. Here a prime denotes a derivative with respect to z, ω_n represents the Matsubara frequency, $\omega_n=(2n+1)(T/T_c)$, $n=0,1,2,\ldots$, and $\Phi_{S,S'}$ is defined by

$$\Phi_{S,S'}=\omega_n F_{S,S'}/G_{S,S'}. \tag{3}$$

In Eqs. (1)–(3), $G_{S,S'}$ and $F_{S,S'}$ are Gorkov's Green functions integrated over energy and averaged over the Fermi surface, which satisfy $G_{S,S'}^2+F_{S,S'}^2=1$.[12] T_c is the transition temperature of the multilayer (or a bilayer, see below). $\Delta_{S,S'}$ and $\xi_{S,S'}$ are the order parameters and coherence lengths, with

$$\xi_{S,S'}=\sqrt{\frac{\hbar D_{S,S'}}{2\pi kT_c}}=\sqrt{\frac{\pi\hbar k}{6e^2\rho_{S,S'}\gamma_{S,S'}T_c}}, \tag{4}$$

where $\rho_{S,S'}$, $D_{S,S'}$, and $\gamma_{S,S'}$ are the resistivities, diffusion coefficients, and coefficients of the normal electronic specific heat, respectively. All the quantities with a unit of energy in Eqs. (1)–(3) have been normalized to πkT_c. To solve these equations, proper boundary conditions should be supplemented, which have the forms[21,10,11]

$$\rho_S G_{S'}^2\Phi_{S'}'=\rho_{S'}G_S^2\Phi_S', \tag{5a}$$

$$R_B G_S\Phi_S'=\rho_S G_{S'}(\Phi_{S'}-\Phi_S), \tag{5b}$$

at the interface $z=0$, where R_B is the specific resistance of the interface (i.e., the product of the interface resistance and its area). At $z=d_{S'}$ and $z=-d_S$, we have[11]

$$\Phi_{S'}'(d_{S'})=0, \tag{6}$$

$$\Phi_S'(-d_S)=0. \tag{7}$$

In principle, Eqs. (1), (2), and (5)–(7), which should be accurate, completely determine the properties of the superconducting multilayers.

In discussing an SS' bilayer in which d_S is large, but $d_{S'}\ll\xi_{S'}$ so that the variation of the order parameters across $d_{S'}$ is small, Golubov *et al.*[10] showed that by taking a slow variation approximation of $\Phi_{S'}$, it is possible to obtain a boundary condition that includes the influences of the S' layer. In this way, a complete solution can be obtained by solving the equations for the S layer alone. Notice that in a bulk superconductor where there is no spatial variation, the second terms on the right-hand sides of Eqs. (1a) and (2a) disappear and we have $\Phi_{S,S'}=\Delta_{S,S'}$, with Eqs. (1b) and (2b) reduced to the usual BCS gap equations. Therefore in Golubov's treatment, Eq. (7) is replaced by $\Phi_S=\Delta_0(T)$ at the thick S layer surface, where $\Delta_0(T)$ is the BCS temperature-dependent energy gap of bulk S material.

We now use the same approximation to Eqs. (1), (2), and (5)–(7) by assuming $d_S\ll\xi_S$. The closed-form equations in the S' region, when we introduce $\theta_{S'}$ function satisfying

$$G_{S'}=\cos\theta_{S'},\quad F_{S'}=\sin\theta_{S'}, \tag{8}$$

can be written as

$$\theta_{S'}''(\omega_n,z)+\Delta_{S'}(z)\cos\theta_{S'}(\omega_n,z)-\omega_n\sin\theta_{S'}(\omega_n,z)=0,$$

$$0\leq z\leq d_{S'}/\xi_{S'}. \tag{9}$$

z is normalized to $\xi_{S'}$. The boundary conditions read

$$\theta'_{S'}(\omega_n, d_{S'}) = 0, \tag{10}$$

$$\theta'_{S'}(\omega_n, 0) = \frac{\gamma_M[\omega_n \sin\theta_{S'}(\omega_n,0) - \Delta_S \cos\theta_{S'}(\omega_n,0)]}{\{1+\gamma_B^2(\omega_n^2+\Delta_S^2)+2\gamma_B[\omega_n\cos\theta_{S'}(\omega_n,0)+\Delta_S\sin\theta_{S'}(\omega_n,0)]\}^{1/2}}, \tag{11}$$

in which γ_B describes the coupling strength, while γ_M is a measure of the strength of the proximity effect, between S and S' layers:[10]

$$\gamma_B = \frac{R_B}{\rho_S\xi_S}\frac{d_S}{\xi_S}, \quad \gamma_M = \frac{\rho_{S'}\xi_{S'}}{\rho_S\xi_S}\frac{d_S}{\xi_S}. \tag{12}$$

The order parameters $\Delta_{S,S'}$ are given by the recurrency expressions

$$\Delta_{S'}^{m+1}(z) = V_{S'}N_{S'}(0)\frac{2T}{T_c}\sum_{\omega_n>0}^{\omega_{D,S'}} F_{S'}^m(\omega_n, z), \tag{13a}$$

$$F_{S'}^m(\omega_n, z) = \sin\theta_{S'}^m(\omega_n, z), \tag{13b}$$

$$\Delta_S^{m+1} = V_S N_S(0)\frac{2T}{T_c}\sum_{\omega_n>0}^{\omega_{D,S}} F_S^m(\omega_n), \tag{14a}$$

$$F_S^m(\omega_n) = \left[1+\left(\frac{\cos\theta_{S'}^m(\omega_n,0)+\gamma_B\omega_n}{\sin\theta_{S'}^m(\omega_n,0)+\gamma_B\Delta_S^m}\right)^2\right]^{-1/2} \tag{14b}$$

in which $\omega_{D,S,S'}$ are Debye frequencies of the individual layers, and $[VN(0)]_{S,S'} = [\ln(T/T_{c,S,S'}) + (2T/T_c)\Sigma_{\omega_n>0}^{\omega_{D,S,S'}}(1/\omega_n)]^{-1}$ are the BCS coupling constants.[13,22] In arriving at Eqs. (9)–(14), the first step is to take the slow gradient approximation of Eq. (2a) and to let $\Phi'_S(z) = \omega_n[\Phi_S(0)-\Delta_S](z+d_S)/\xi_S^2 G_S(0)$, which automatically satisfies Eq. (7). Δ_S is considered to be space independent. From this and Eq. (5b), one obtains $\Phi_S(0)$ expressed in terms of the quantities in the S' region and of Δ_S. One further assumes a space independent $\Phi_S(z) = \Phi_S(0)$. Inserting it into Eq. (2b) leads to Eq. (14). Further, from Eq. (5a) and the obtained expressions, we can derive Eq. (11). Equations (9), (10), and (13) are Eqs. (1a), (6), and (1b) rewritten in terms of $\theta_{S'}$, respectively.

We note that one of the main differences between the present formalism and that of Ref. 10 is reflected in the boundary condition Eq. (10), since if we interchange the subscripts S and S', Eqs. (9)–(14) will essentially be identical to those of that reference except that this condition is replaced by $\theta_S(\omega_n, d_S\to\infty) = \arctan[\Delta_0(T)/\omega_n]$. This arises directly from the thick S layer considered there, which is the opposite of our case. An important consequence of this difference is that T_c no longer equals $T_{c,S}$, but may vary between $T_{c,S'}$ and $T_{c,S}$ in our case. In addition, the boundary conditions given in Eqs. (6) and (7) are more general in a sense that they should apply both to SS' multilayer systems (due to symmetry) or to an *isolated* SS' bilayer (due to its free surfaces at $z = d_{S'}$ and $-d_S$) (see Fig. 1). Hence our formalism applies, and the following results should be true, in both cases.

To solve the system of Eqs. (9)–(14), which are the basic equations for the following calculations, we begin by using certain starting values of $\Delta_{S,S'}$ and $\theta_{S'}$ and Eqs. (9)–(11) are solved numerically. The resulting $\theta_{S'}$ is inserted into Eqs. (13) and (14) to calculate $\Delta_{S,S'}$, which are used for solving Eqs. (9)–(11) again. This proceeds until a satisfactory accuracy is reached. In the calculations, the input parameters required are $\omega_{D,S}$, $\omega_{D,S'}$, $T_{c,S}$, $T_{c,S'}$, $d_{S'}$, γ_B, and γ_M.

III. TRANSITION TEMPERATURE

Since we have $T_{c,S'} < T_c < T_{c,S}$ in general, T_c needs to be calculated first for given input parameters. One way for doing this is to set T_c equal to T in Eqs. (13a) and (14a). Then, by solving the system of equations, the order parameter Δ_S ($>\Delta_{S'}$) is found to decrease monotonically with increasing T, and T_c can be defined as T at which Δ_S vanishes. The typical $T_c \sim d_{S'}$ curves are shown in Fig. 2, taking Nb/Al multilayers as an example. In the calculations, we have taken $\omega_{D,Nb} = 275$ K, $\omega_{D,Al} = 428$ K. Bulk values of $T_{c,Nb} = 9.2$ K and $T_{c,Al} = 1.2$ K were also used regardless of their possible suppression with Nb layer thickness $\sim 2\xi_{\mathrm{Nb}}$ and with smaller d_{Al}. As can be seen in the figure, T_c increases with the increase of γ_M and of γ_B. It tends to $T_{c,Nb}$ as $d_{Al}\to 0$, and is almost constant for d_{Al} above 2 or $3\xi_{Al}$, as expected.

Another way for evaluating T_c from the Usadel equations, which is actually applicable for dirty SS' multilayers with arbitrary values of both d_S and $d_{S'}$, has been proposed by Biagi, Kogan, and Clem[23] for the case of zero interface re-

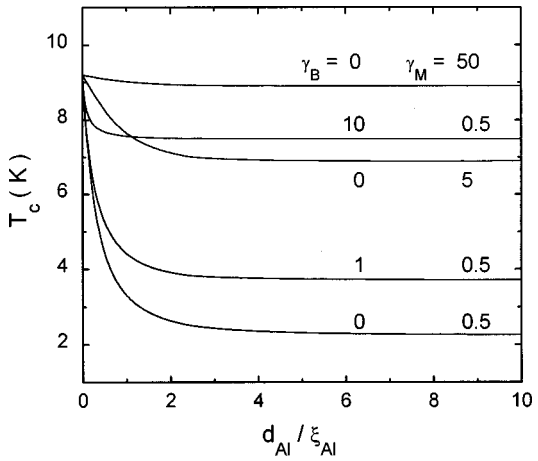

FIG. 2. Transition temperature T_c vs d_{Al}/ξ_{Al} for Nb/Al layered systems. We have assumed $d_{Nb} \sim \xi_{Nb}$, $T_{c,Al} = 1.2$ K, and $T_{c,Nb} = 9.2$ K. See text for other material parameters.

sistance R_B. The basic idea is that near T_c, one has $G_{S,S'} \to 1$, and $F_{S,S'}$, $\Delta_{S,S'} \to 0$ so that Eqs. (1a) and (2a) can be linearized with respect to $F_{S,S'}$:

$$-\frac{\hbar D_{S'}}{2\pi k T_c} F''_{S'} = \Delta_{S'} - \omega_n F_{S'}, \tag{15a}$$

$$-\frac{\hbar D_S}{2\pi k T_c} F''_S = \Delta_S - \omega_n F_S. \tag{15b}$$

Since both $F_{S,S'}$ and $\Delta_{S,S'}$ vanish near T_c, we assume a solution of the form

$$F_{S,S'} = \frac{\Delta_{S,S'}}{\omega_n + (T/T_c)\delta_{S,S'}}. \tag{16}$$

Inserting these into Eqs. (1b) and (2b), we find that $\delta_{S,S'}$ are determined by the following expressions:

$$\ln\left(\frac{T}{T_{c,S'}}\right) = -2\sum_{n\geqslant 0}\left(\frac{1}{2n+1} - \frac{1}{2n+1+\delta_{S'}}\right), \tag{17a}$$

$$\ln\left(\frac{T}{T_{c,S}}\right) = -2\sum_{n\geqslant 0}\left(\frac{1}{2n+1} - \frac{1}{2n+1+\delta_{S}}\right). \tag{17b}$$

The boundary conditions between S and S', now with $R_B \neq 0$, are Eq. (5), which can be written in terms of $F_{S,S'}$ as

$$\rho_{S'} F'_S = \rho_S F'_{S'}, \tag{5a'}$$

$$F_S - F_{S'} = (R_B/\rho_{S'}) F'_{S'}. \tag{5b'}$$

Using these relations, one is able to obtain the following simple transcendental equation governing T_c:[23]

$$\rho_S q_{S'} \tanh(q_{S'} d_{S'}) - \rho_{S'} q_S \tan(q_S d_S) = R_B q_S q_{S'} \tanh(q_{S'} d_{S'}) \tan(q_S d_S), \tag{18}$$

in which $q_{S,S'}$ are given by

$$q^2_{S'} = -\frac{2\pi k T \delta_{S'}}{\hbar D_{S'}}, \tag{19a}$$

$$q^2_S = \frac{2\pi k T \delta_S}{\hbar D_S}. \tag{19b}$$

Equations (17)–(19) can be used to evaluate T_c for any SS' systems if the parameters of $T_{c,S,S'}$, $\rho_{S,S'}$, $d_{S,S'}$, and R_B are known,[24] and they reduce to the well-known results of de Gennes and Werthamer[8,25,26] when $R_B = 0$. Moreover, since they are derived directly from Eqs. (1), (2), and (5), the method is therefore accurate. We have compared the T_c data evaluated in the above two different ways. We found that when d_S is smaller than ξ_S, say, $d_S = \xi_S/5$, the two methods produce basically the same results with discrepancies below 0.5%, which is largely due to the accuracy we adopted in the calculations. When $d_S = \xi_S$, the discrepancy increases to 1 $\sim$1.5%. These results indicate that Eqs. (9)–(14) are a reasonable thin S layer approximation from the original Usadel equations, which could have an acceptable accuracy for d_S as large as ξ_S. Since in this work we are mainly interested in the influence of the S' layers on $\lambda(T)$, we shall for simplicity fix the S layer parameters, and take $d_S = \xi_S$. Using Eqs. (12) and (4), we have

$$\gamma_B = \frac{R_B}{\rho_S \xi_S}, \quad \gamma_M = \sqrt{\frac{\rho_{S'}\gamma_S}{\rho_S \gamma_{S'}}}. \tag{20}$$

These simpler expressions will be used in the following numerical calculations.

IV. PENETRATION DEPTHS

With known T_c, other superconducting quantities for the given bilayer or multilayer system can be obtained by solving Eqs. (9)–(14). In this section, we derive the formulas for the in-plane and out-of-plane penetration depths. We then present some typical results for the Nb/Al and Nb/Cu layered systems.

Since $F_{S,S'}$ are real quantities in our case, the current density is directly proportional to the vector potential,[12] i.e., we have $\boldsymbol{J} = -(1/\mu_0\lambda^2)\boldsymbol{A}$, with

$$\frac{1}{\lambda^2_{S,S'}} = \frac{\mu_0 e^2 n_{S,S'}}{m} = \frac{2\pi\mu_0 k T}{\hbar \rho_{S,S'}} \sum_{\omega_n > 0}^{\omega_{D,S,S'}} |F_{S,S'}|^2, \tag{21}$$

where $n_{S,S'}$ are the superfluid densities, $F_{S,S'} = \sin\theta_{S,S'}$ represent the end results of Eqs. (13b) and (14b) (removing all superscripts). Equation (21) defines the local $\lambda_{S,S'}$ and $n_{S,S'}$ that vary along the z axis. The in-plane penetration depth $\lambda_{ab}(T)$ is related to the areal superfluid densities $\int n_{S,S'} dz$, and is given by

$$\lambda^2_{ab}(T) = \frac{d_S + d_{S'}}{\int_{-d_S}^{d_{S'}} \lambda^{-2}(T,z) dz}, \tag{22}$$

in which λ is given by Eq. (21). To evaluate the out-of-plane component $\lambda_c(T)$, we follow Clem and Coffey,[27] and consider an infinite slab of multilayer, as shown in Fig. 1, with its thickness $w \gg \lambda$, and with an external magnetic field B_y applied along the y axis. In this geometry, there exist supercurrents J_z along the z axis near the surfaces of the slab. If we assume $\lambda \gg d_{S,S'}$, B_y and J_z will approximately be the functions of x only. If we make a contour C, the magnetic flux within C is $(d_S + d_{S'})\int_0^x B_y(x')dx' = \int_C \mathbf{A}\cdot d\mathbf{l}$. Using London's equation and Ampere's law, and differentiating with respect to x, we are led to $B_y = \lambda_c^2(\partial^2 B_y/\partial x^2)$, with

$$\lambda^2_c(T) = \frac{\int_{-d_S}^{d_{S'}} \lambda^2(T,z) dz}{d_S + d_{S'}}. \tag{23}$$

Figure 3 shows the calculated results of $\lambda_{ab}(T)$ and $\lambda_c(T)$ for Nb/Al (solid lines) and Nb/Cu (dashed lines) systems in the temperature range below $0.92T_c$. In Fig. 4, the low-temperature region of $\lambda_{ab}(T)$ is plotted. For the calculation of these data, we used $\omega_{D,Cu} = 343$ K, and instead of the experimental value of $T_{c,Cu} = 0$ K, we used the theoretical value of $T_{c,Cu} = 0.015$ K,[28] which is close to 0 K and makes our model applicable. γ_{Nb}, γ_{Al}, and γ_{Cu} were taken to be

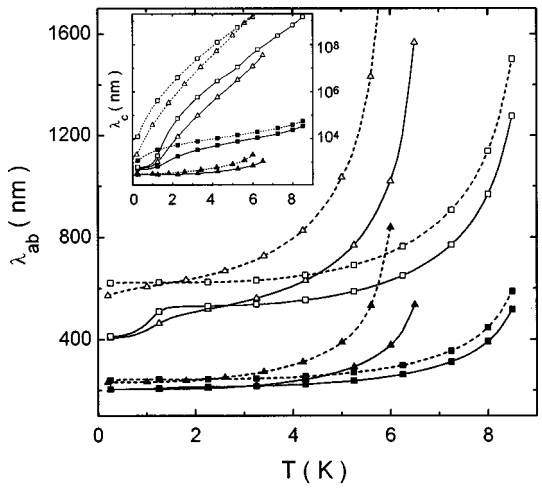

FIG. 3. Calculated $\lambda_{ab}(T)$ for Nb/Al (solid curves) and Nb/Cu (dashed curves) layered structures. Open symbols: $d_{S'}/\xi_{S'}=20$; solid symbols: $d_{S'}/\xi_{S'}=2.5$. Triangles: $\gamma_B=0$, $\gamma_M=5$; squares: $\gamma_B=270$, $\gamma_M=5$. The inset shows the corresponding data of $\lambda_c(T)$. See text for other material parameters.

7.3, 1.36, and 0.97×10^{-4} J/cm^3 K^2, respectively. $\rho_{Nb}=5\mu\Omega$ cm was also used, while ρ_{Al} and ρ_{Cu} were calculated from Eq. (20) for given γ_M values. From Figs. 3 and 4, we can see that, depending on $d_{S'}$, $T_{c,S'}$, and γ_B, the form of

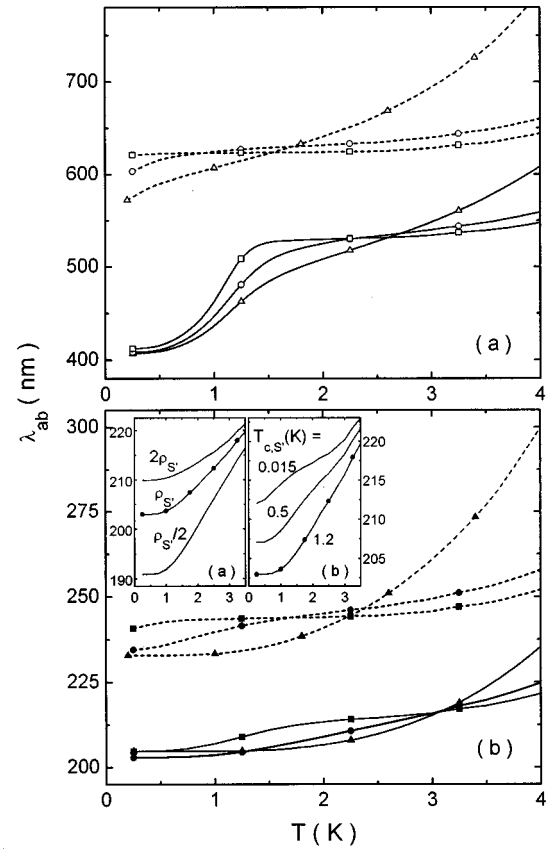

FIG. 4. Low-temperature part of $\lambda_{ab}(T)$ of Fig. 3: (a) $d_{S'}/\xi_{S'}=20$, (b) $d_{S'}/\xi_{S'}=2.5$. Results for $\gamma_B=50$, $\gamma_M=5$ are added (circles). The curve for $\gamma_B=50$, $\gamma_M=5$, $d_{S'}/\xi_{S'}=2.5$ is also plotted in the insets, and the variations with $\rho_{S'}$ and $T_{c,S'}$ are shown in insets (a) and (b), respectively.

$\lambda(T)$ curves is very much varied. If we fit the data $\Delta\lambda(T)/\lambda(0)$ in the lowest temperature region ($\leqslant 1$ K) with a power law αT^{β}, we find that β would range from 1–6 for $\lambda_c(T)$. For $\lambda_{ab}(T)$, our fit also leads to the power law in most cases, and an exponential behavior is obtained if $T_{c,S'}$ is well above 1 K.

In the temperature region below $3\sim4$ K, we mention two interesting features of the $\lambda_{ab}(T)$ data that result from the calculations. First of all, a two-gap-like $\lambda_{ab}(T)$ can be seen clearly in Fig. 4(a) for Nb/Al system with largest γ_B and d_{Al} (solid line plus open squares). As γ_B decreases, such feature becomes less clear, and so it does when d_{Al} is smaller, as can be seen in Fig. 4(b). These might be anticipated from a simple physical consideration since for weaker Nb/Al interlayer coupling and larger d_{Al}, there will be larger volume of Al that is less affected by Nb, which therefore contributes more to the decrease of $\lambda_{ab}(T)$ around $T_{c,Al}$. In the region near $T_{c,Al}$ where a faster decrease occurs, the $\lambda_{ab}(T)$ curve shows a sublinear temperature dependence. This is the case also for the Nb/Cu system, as demonstrated by some of the dashed curves in Fig. 4. All these results seem to be consistent with the data experimentally obtained by Pambianchi and co-workers in Nb/Al (Ref. 1) and Nb/Cu (Ref. 2) bilayers and the data obtained in NbN/Al and Nb/Cu bilayer systems by Claassen *et al.*[3]

A second interesting feature from the calculation is that in some parameter range, the $\lambda_{ab}(T)$ curve shows a linear temperature dependence, and with decreasing temperature it switches to a power law around $T_{c,S'}$. To see this more clearly, we plot the $\lambda_{ab}(T)$ curve of solid line plus solid circles in Fig. 4(b) again in the insets. $\lambda_{ab}(T)$ is shown to decrease linearly from about 3.5–1.2 K, below which it switches to a power law with $\beta\sim3$. In inset (a), we see that changing $\rho_{S'}$ [from Eq. (20), it means changing γ_M with other parameters fixed] results in the change of α, but not β. In inset (b), the effect of changing $T_{c,S'}$ is shown. In this case, α and β and the point at which the curve switches from linear to power law will all change. For $T_{c,S'}=0.5$ and 0.015 K, β equals 2.3 and 2 approximately.

V. DISCUSSIONS

A. Comparison with phenomenological model

The rich characteristics in the $\lambda(T)$ data are a result of the spatial variations of the superconducting properties, as mentioned earlier. In Ref. 7, Pambianchi, Mao, and Anlage proposed a phenomenological approach to evaluate $\lambda(T)$ that utilizes a space- and temperature-dependent order parameter. Their model I considers an active S' (or N) layer in screening due to proximity effect, while the S layer is unaffected by the presence of the S' (or N) layer. The situation is actually what we are considering in the present work if we simply approximate $\Delta_S(T)$ to $\Delta_0(T)$ in our formalism [Eq. (14) can be removed under this approximation].[29] Their model II, on the other hand, considers an opposite case in which the N layer has a zero pair potential, and the S layer suffers a suppressed order parameter within a distance of $\sim\xi_S$ near the interface. This model is similar to the situation Golubov *et al.* discussed for an SN bilayer.[30,31] We now discuss in further detail their model I, in which the order parameter has the form

$$\Delta_{S'}(z,T)\sim \frac{V_{S'}}{V_S}\frac{\Delta_0(T)}{\Delta_0(0)}e^{-Kz}, \tag{24}$$

where $V_{S,S'}$ are the BCS coupling constants for individual S and S' layers, and $K^{-1}=K_{S'}^{-1}$ is the decay length in the S' layers which is given by

$$\ln\left(\frac{T}{T_{c,S'}}\right)=\psi\left(\frac{1}{2}\right)-\psi\left(\frac{1}{2}-\frac{\hbar D_{S'}K^2}{4\pi kT}\right) \tag{25}$$

for $T>T_{c,S'}$, where ψ is the digamma function, and by

$$K^{-1}=\sqrt{\frac{\hbar D_{S'}}{2\pi kT}}=\frac{\xi_{S'}}{\sqrt{t}}, \quad t=T/T_c \tag{26}$$

for $T_{c,S'}=0$. It is obvious that Eq. (25) is simply Eq. (17a) with

$$\delta_{S'}=\frac{K^2\xi_{S'}^2}{t}. \tag{27}$$

The order parameter described by Eq. (24) has the exponential decay characteristics in the space variations. The decay lengths from Eqs. (25) and (26), when normalized to $\xi_{S'}$, are, respectively,

$$\frac{K^{-1}}{\xi_{S'}}=\frac{1}{\sqrt{\delta_{S'}t}}, \tag{28a}$$

$$\frac{K^{-1}}{\xi_{S'}}=\frac{1}{\sqrt{t}}. \tag{28b}$$

The temperature variations, on the other hand, arise from the BCS temperature-dependent energy gap as well as the decay length as expressed in Eq. (28).

Pambianchi's model is found to explain successfully the experimental data on Nb/Al and Nb/Cu systems to a temperature as low as 2 K.[1,2] It will therefore be interesting to compare our results with their model. In Fig. 5, we show the semilog plot of the spatial variations of the order parameter, as given by Eq. (13), at several reduced temperatures for a Nb/Al structure with vanishing interface resistance R_B. We see that near T_c, the order parameter shows a nice exponential decay behavior over a large distance, as described by Eq. (24), except for the boundary regions ($\sim\xi_{Al}$) next to $z=0$ and $z=20\xi_{Al}$. With decreasing temperature, these regions expand, and at low temperatures the decay is no longer exponential and is much slower. If we take the distances across which the order parameters decrease to e^{-1} of their initial values at $z=0$ for the decay lengths, they would vary with temperature as is shown in the inset of Fig. 5 (solid squares). The solid and dashed lines in the inset are the decay lengths from Eqs. (28a) and (28b), with $\delta_{S'}$ computed from Eq. (17a) for given $T_{c,S'}$. While the two curves both tend to infinite mathematically when T approaches $T_{c,S'}$ and zero, the latter appears to be closer to our results as a whole.

Results plotted in Fig. 5 were obtained with the parameters $\gamma_B=0$, $\gamma_M=5$, and $d_{Al}/\xi_{Al}=20$, and they are rather general. From the figure, we can see an important, qualitative difference predicted by different models. The results from

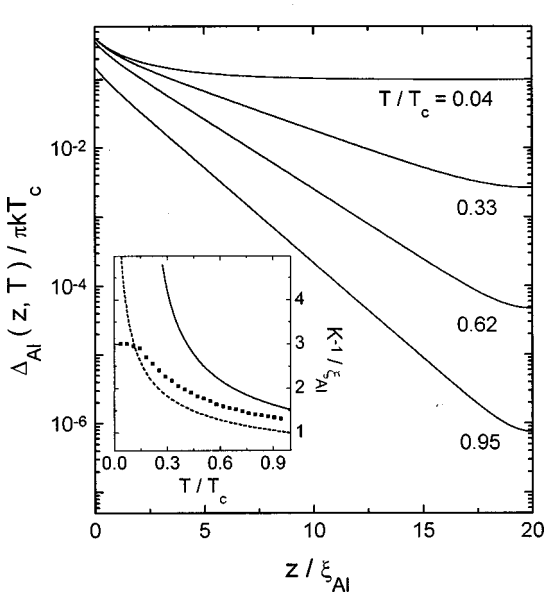

FIG. 5. Space dependence of Δ_{Al} for several reduced temperatures in the case of $\gamma_B=0$, $\gamma_M=5$, and $d_{Al}/\xi_{Al}=20$. An exponential decay can be seen over a large portion across d_{Al} provided that the temperature is not very low. The decay length K^{-1}, taken as the distance across which Δ_{Al} drops to e^{-1} of its initial value at $z=0$, is plotted in the inset as solid squares. The solid and dashed lines in the inset are calculated according to Eqs. (28a) and (28b), respectively.

Eq. (28) indicate that the decay length is divergent as T approaches $T_{c,S'}$ or zero. This has been discussed in detail in the case of Nb/Cu bilayer systems.[2] However, this divergent behavior does not appear in our calculations, as can be seen from Eq. (13) that $\Delta_{S'}$ is expected to change smoothly as T turns around $T_{c,S'}$. Although it is well known that the coherence length for a bulk material diverges near its transition temperature, which is typical of the second-order phase transition in the Ginzburg-Landau theory,[9] it is less clear whether the decay length should be the case as T tends to $T_{c,S'}$ or 0 for the spatially inhomogeneous SS' or SN structures, since Eqs. (25) and (26) are derived from the linearized self-consistency equation valid only for temperatures near T_c.[8] In fact, Eq. (25) is derived again in Sec. III from Eq. (1b) under the small $\Delta_{S'}$ approximation near T_c. The picture resulting from our calculations is that with decreasing temperature, the decay gradually deviates from the exponential behavior, and becomes very slow at low temperatures so that the influence of the S layer on the S' or N layer can extend to a large distance away from the interface, which is consistent with the experimental observations.

In Fig. 6 the temperature dependences of the order parameters at several positions are shown (solid lines). The dotted line shows the data in the Nb layers, which is space independent. The dashed lines are the results from Eq. (24), with the coefficient set to match the data at $z/\xi_{Al}=T/T_c=0$, while K^{-1} is given by Eq. (28b). According to Eq. (24), the temperature dependence of the order parameter at $z=0$ is that of the rescaled BCS energy gap $\Delta_0(T)$. Our data, Δ_{Al} near $z=0$ and Δ_{Nb}, follow closely such a dependence, as is seen in Fig. 6. As z increases, the order parameter decreases faster with increasing temperature than expected from $\Delta_0(T)$,

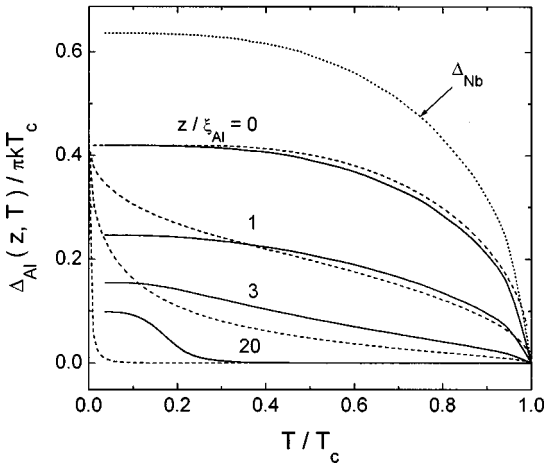

FIG. 6. Temperature dependences of Δ_{Nb} (dotted line), and Δ_{Al} (solid line) at several positions across d_{Al} for the parameters of $\gamma_B=0$, $\gamma_M=5$, and $d_{Al}/\xi_{Al}=20$. The dashed lines are computed according to Eqs. (24) and (26) by adjusting the coefficient in Eq. (24) to match the solid curve at $T/T_c=z/\xi_{Al}=0$.

which is realized by a temperature-dependent decay length K^{-1} in Eq. (24). From Fig. 6 we can see that our results and those from Pambianchi's model give basically the same trends of the temperature dependences of the order parameters. At low temperatures, however, the deviations are considerable. As $T\rightarrow 0$, all the dashed curves approach $\Delta_{Al}(0,0)$, due to the fact that $K^{-1}\rightarrow\infty$ in this limit.

The inverse of the space- and temperature-dependent penetration depth $\lambda_{Al}(z,T)$, computed from Eq. (21) for the same parameters is shown in Fig. 7. The λ_{Al}^{-1} data display quite similar features as Δ_{Al} shown in Fig. 6. In Ref. 1, a simple way using $\lambda^{-1}\sim\Delta$ is employed to fit the Nb/Al data. The dashed lines are plotted in this way with Δ_{Al} calculated from Eq. (24). Again the coefficient is chosen so that the two sets of data coincide at $z/\xi_{Al}=T/T_c=0$.

From the discussions above, we may conclude that our model and Pambianchi's model can lead to similar results so

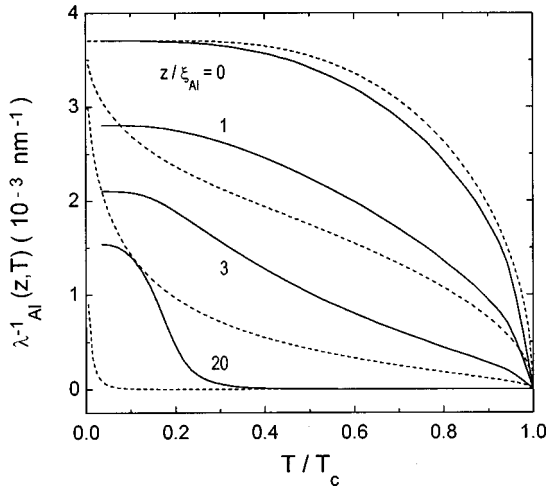

FIG. 7. Temperature dependences of λ_{Al}^{-1} at several positions across d_{Al} in the case of $\gamma_B=0$, $\gamma_M=5$, and $d_{Al}/\xi_{Al}=20$. The dashed lines are from the simple relation $\lambda^{-1}\sim\Delta_{Al}$, computed according to Eqs. (24) and (26) by adjusting the coefficient in Eq. (24) to match the solid curve at $T/T_c=z/\xi_{Al}=0$.

far as the temperature is not very low. These include the exponential decay characteristics with a decay length K^{-1} and space- and temperature-dependent superconducting properties like the order parameters and penetration depths. In the low-temperature region, however, the predictions from the two models are qualitatively different. Further experiments will be required in testing the model predictions in this temperature region.

B. Highly anisotropic multilayers and high-T_c superconductors

High-T_c superconductors are intrinsically layered materials which usually have highly anisotropic properties (in-plane vs out-of-plane).[14] Experimental measurements of the penetration depth on these materials have revealed a variety of temperature dependences. Some experiments indicate a two-gap-like,[32] or an exponential, behavior.[33] Most experiments show that $\lambda_c(T)$ obeys a power law,[34] whereas $\lambda_{ab}(T)$ is linear and quadratic at low and very low temperatures,[15,16] which is often interpreted in terms of impurity scattering[17] or nonlocal effects[18] within the framework of *d*-wave superconductivity. In addition to the *d*-wave pairing symmetry, Adrian *et al.*[19] and Klemm and Liu[20] demonstrated the importance of the proximity effect by considering a multilayer system consisting of one *S* and one *N* layer per unit cell. They concluded that the exponential or power law[19] and linear behavior[20] can be produced, provided that the proximity-coupled *N* layers are taken into account. As can be seen in the previous section, our results support this picture. In addition we have taken into account the finite thickness of the S' layers, and their material parameters. We see that many of our results mimic those observed experimentally in the high-T_c cuprates, although the work is based upon the simple *s*-wave superconductivity, which alone can hardly be the case for the cuprates.

We point out that an SS' multilayer with anisotropies as large as the cuprates will usually have the parameters out of the range in which the distinct features like the linear plus quadratic behavior in $\lambda_{ab}(T)$ appear. This can be seen in the following way. For a multilayer in Fig. 1, the macroscopic sample resistivities $\rho^{\perp}$ and $\rho^{\parallel}$ can be easily shown to be related to $\rho_{S,S'}$, $d_{S,S'}$ and R_B as

$$\rho_S d_S+\rho_{S'}d_{S'}+R_B=\rho^{\perp}(d_S+d_{S'}), \tag{29}$$

$$\rho_S\rho_{S'}(d_S+d_{S'})=\rho^{\parallel}(\rho_S d_{S'}+\rho_{S'}d_S). \tag{30}$$

Here $R_B=\gamma_B\rho_S d_S$. For high-T_c materials, $\rho^{\perp}/\rho^{\parallel}$ ranges from 40 to 8×10^5.[14] With this large anisotropy, Eqs. (29) and (30) would yield large γ_B or $\rho_{S'}$ (we assume $\rho_{S'}>\rho_S$), which from Eq. (20) means large γ_M, and from Eq. (21) reduces S' layer contribution to $\lambda(T)$. If we take $2d_{S'}/2d_S=8.4\ \text{Å}/3.34\ \text{Å}=2.5$, and the lowest ratio $\rho^{\perp}/\rho^{\parallel}=40$ for YBCO,[14] for example, we have $\gamma_B=270$ and $\rho_{S'}/\rho_S=3.31$ or $\gamma_B=0$ and $\rho_{S'}/\rho_S=193$. According to our results, these will already make the linear plus quadratic feature disappear altogether. Hence for a multilayer with high $\rho^{\perp}/\rho^{\parallel}$ ratio, usually two limiting cases are expected in the $\lambda_{ab}(T)$ characteristics. One is a clear two-gap structure (for large γ_B values), the other is a nearly exponential behavior of a single BCS superconductor (for large $\rho_{S'}$ values). The possibility of having a ''nontrivial'' $\lambda_{ab}(T)$ characteristic in the highly aniso-

tropic multilayers exists if they are composed of certain kind of bilayers or structures (for instance, the region between $z=-2d_S-d_{S'}$ and $z=d_{S'}$ in Fig. 1) as unit cells, and high $\rho^{\perp}/\rho^{\parallel}$ ratios are attributed to additional, stronger barriers between these unit cells, which do not necessarily enter into the calculation. Under the circumstances, a different $\lambda_c(T)$, as compared to that of Eq. (23), will result.

VI. SUMMARY

We have calculated the penetration depths $\lambda(T)$ of conventional SS' ($T_{c,S}>T_{c,S'}$) layered superconductors which contain both multilayers and bilayers. The SN structures have been discussed in the limit of $T_{c,S'}\to 0$. The variations of the parameters of the S' layers, which include the transition temperature, layer thickness, and resistivity, as well as their coupling strength to the S layers, are considered. These factors influence in many ways the space and temperature variations of the order parameters, which give rise to a variety of temperature dependences of $\lambda(T)$. Many basic features experimentally observed, like the linear, sublinear, or power-law dependences, have been reproduced.

Our calculations are based upon Usadel's quasiclassical equations, which are the dirty-limit version of Eilenberger's theory. The approach is therefore applicable to the dirty SS' systems. Although we have obtained in this paper a simple transcendental equation for the evaluation of the transition temperature, which is rather general for arbitrary individual layer thicknesses and can reduce to the well-known results of de Gennes and Werthamer for zero interface resistance, the rest of the calculations have been made on the thin S layer approximation $d_S \leqslant \xi_S$. This may be the main constraint on applying the approach to the real systems. However, the present model can be useful in describing the superconducting properties of the SS' layered systems in the whole temperature range below T_c. In this paper, we have compared our model with the phenomenological model of Pambianchi *et al.* which is valid strictly near T_c. We find that the two models yield results that are very similar if the temperature is not low (say, $T>0.3T_c$), but in the low-temperature region, the results differ considerably. We note that in Pambianchi's model, the order parameter of the S layer is approximated by its bulk value $\Delta_0(T)$. If we use the same approximation, the boundary problem Eqs. (9)–(11) can be solved with $\Delta_{S'}$ given by Eq. (13) and Δ_S by $\Delta_0(T)$, and Eq. (14) is not required.

Within our formalism, $\lambda(T)$ can be accurately determined if the material parameters like the transition temperatures, Debye frequencies, coefficients of the electronic specific heat, and resistivities, and sample parameters like the individual layer thicknesses and specific resistance of the interface are known. This would allow for a quantitative comparison between our model and experimental observations. Of particular interest will be the $\lambda(T)$ characteristics under the variation of these parameters in the low-temperature region. Further experimental work will be required in these studies.

ACKNOWLEDGMENT

We thank R. F. Wang for helpful discussions during the early stage of this work.

[1] M. S. Pambianchi, S. N. Mao, and S. M. Anlage, Phys. Rev. B **52**, 4477 (1995).

[2] M. S. Pambianchi, L. Chen, and S. M. Anlage, Phys. Rev. B **54**, 3508 (1996).

[3] J. H. Claassen, J. E. Evetts, R. E. Somekh, and Z. H. Barber, Phys. Rev. B **44**, 9605 (1991).

[4] R. W. Simon and P. M. Chaikin, Phys. Rev. B **30**, 3750 (1984); **23**, 4463 (1981).

[5] K. Kanoda, H. Mazaki, N. Hosoito, and T. Shinjo, Phys. Rev. B **35**, 8413 (1987).

[6] ac susceptibility, two-coil mutual inductance, and microwave surface impedance measurements are used to determine $\lambda(T)$. These measurements all employ ac signals with frequencies ranging from 10^2–10^{10} Hz. However, the experimental data obtained are, or can be explained by, a frequency-independent (dc) penetration depth, which is also what we consider in this paper. See Refs. 1–3 and 5 for further details.

[7] M. S. Pambianchi, J. Mao, and S. M. Anlage, Phys. Rev. B **50**, 13 659 (1994).

[8] G. Deutscher and P. G. de Gennes, in *Superconductivity*, edited by R. D. Parks (Marcel Dekker, New York, 1969).

[9] P. G. de Gennes, *Superconductivity of Metals and Alloys* (Benjamin, New York, 1966).

[10] A. A. Golubov, E. P. Houwman, J. G. Gijsbertsen, V. M. Krasnov, J. Flokstra, H. Rogalla, and M. Yu. Kupriyanov, Phys. Rev. B **51**, 1073 (1995).

[11] A. A. Golubov, Proc. SPIE **2157**, 353 (1994).

[12] K. Usadel, Phys. Rev. Lett. **25**, 507 (1970).

[13] G. Eilenberger, Z. Phys. **214**, 195 (1968).

[14] S. L. Cooper and K. E. Gray, in *Physical Properties of High Temperature Superconductors*, edited by D. M. Ginsberg (World Scientific, Singapore, 1994).

[15] W. N. Hardy, D. A. Bonn, D. C. Morgan, Ruixing Liang, and Kuan Zhang, Phys. Rev. B **70**, 3999 (1993).

[16] D. A. Bonn, S. Kamal, Kuan Zhang, Ruixing Liang, D. J. Baar, E. Klein, and W. N. Hardy, Phys. Rev. B **50**, 4051 (1994).

[17] P. J. Hirschfeld and N. Goldenfeld, Phys. Rev. B **48**, 4219 (1993).

[18] I. Kosztin and A. J. Leggett, Phys. Rev. Lett. **79**, 135 (1997).

[19] S. D. Adrian, M. E. Reeves, S. A. Wolf, and V. Z. Kresin, Phys. Rev. B **51**, 6800 (1995).

[20] R. A. Klemm and S. H. Liu, Phys. Rev. Lett. **74**, 2343 (1995).

[21] M. Yu. Kuprianov and V. F. Lukichev, Zh. Éksp. Teor. Fiz. **94**, 139 (1988) [Sov. Phys. JETP **67**, 1163 (1988)].

[22] Since we have $(2T/T_c)\Sigma_{\omega_n>0}^{\omega_{D,S,S'}}(1/\omega_n)=\ln(1.14\Omega_{D,S,S'}/kT)$, here $\Omega_{D,S,S'}=kT_c\omega_{D,S,S'}$, $\ln(T/T_{c,S,S'})+(2T/T_c)\Sigma_{\omega_n>0}^{\omega_{D,S,S'}}(1/\omega_n)$ can be expressed as $\ln(1.14\Omega_{D,S,S'}/kT_{c,S,S'})$, which is simply $[VN(0)]_{S,S'}^{-1}$. For the first equality, see for example, P. G. de Gennes, Rev. Mod. Phys. **36**, 225 (1964).

[23] K. R. Biagi, V. G. Kogan, and J. R. Clem, Phys. Rev. B **32**, 7165 (1985).

[24] We have not included the terms of perpendicular upper critical

field H_{c2} in Eqs. (20). However, this can be easily done, so the present formalism can be used to extend the discussions of Ref. 23 on H_{c2} to the SS' systems with nonzero interface resistance.
[25] P. G. de Gennes and E. Guyon, Phys. Lett. **3**, 168 (1963).
[26] N. R. Werthamer, Phys. Rev. **132**, 2440 (1963).
[27] J. R. Clem and M. W. Coffey, Phys. Rev. B **42**, 6209 (1990).
[28] R. Meservey and B. B. Schwartz, in *Superconductivity*, edited by R. D. Parks (Marcel Dekker, New York, 1969).
[29] From our numerical calculations, a self-consistent solution can be obtained under this approximation. Physically, however, $\Delta_S(T)$ should always be smaller than $\Delta_0(T)$ due to the presence of the S' layer.
[30] A. A. Golubov and M. Yu. Kupriyanov, J. Low Temp. Phys. **70**, 83 (1988).
[31] S. P. Zhao, F. Finkbeiner, Ph. Lerch, A. Zehnder, and H. R. Ott, J. Low Temp. Phys. **93**, 641 (1993).
[32] N. Klein, N. Tellmann, H. Schulz, K. Urban, S. A. Wolf, and V. Z. Kresin, Phys. Rev. Lett. **71**, 3355 (1993).
[33] D. H. Wu, J. Mao, S. N. Mao, J. L. Peng, X. X. Xi, T. Venkatesan, R. L. Greene, and S. M. Anlage, Phys. Rev. Lett. **70**, 85 (1993).
[34] C. Panagopoulos, J. R. Cooper, T. Xiang, G. B. Peacock, I. Gameson, and P. P. Edwards, Phys. Rev. Lett. **79**, 2320 (1997).